measurement was set 100 Hz upfield of the resonance being analyzed; τ-values ranged from 0.001 to 120 s, and good S/N ratios were achieved within 20-60 scans.

The long $T1$ values for **1** prohibited the rapid data collection needed to follow the scrambling process. In order to accelerate relaxation all kinetic NMR measurements were performed with a pulse width of 60 μs and with solutions 0.06 M **1** in $CDCl_3$ containing 0.05 M $Cr(acac)_3$ as a PARR. The presence of the PARR produced only very minor changes in chemical shifts and line widths, and allowed pulse delays to be reduced to 5 s. To ensure that differences in relaxation rates (see $T1$ values in Table IV were still not biasing the eigenintensities $Q1$ and $Q2$, the relative intensities of the three signals at $t = \infty$ were used to obtain numerical factors (ideally 2:2:1 for N1,2:N3,4:N5) needed for normalization of the kinetic data. S/N ratios of 60 were obtained within 250 or 450 scans. Over the temperature range 5-30 °C, the decay of $Q1$ and growth in $Q2$ could be reliably monitored for at least six half-lives, ie., 9.5 h at 5 °C and 2.0 h at 30 °C.

Molecular Orbital Calculations. MNDO calculations of charge densities and bond orders in EN_5S_3 structures were performed using the MOPAC suite of programs[26] operating on a SUN/3 workstation. The calculations were performed with full geometry optimization within a C_s symmetry constraint.

Acknowledgment. We thank the Natural Sciences and Engineering Research Council of Canada for financial support and an NSERC postdoctoral fellowship (to R.T.B.).

Appendix

Treatment of Kinetic Data. Combination of the two sets of coupled first-order processes shown in Scheme IV gives rise to the following secular determinant:[9]

$$\begin{vmatrix} -2(k_c+k_s)-\lambda & k_s & k_c & 0 & (k_c+k_s) \\ k_s & -2(k_c+k_s)-\lambda & 0 & k_c & (k_c+k_s) \\ k_c & 0 & -2(k_c+k_s)-\lambda & (k_c+2k_s) & 0 \\ 0 & k_c & (k_c+2k_s) & -2(k_c+k_s)-\lambda & 0 \\ (k_c+k_s) & (k_c+k_s) & 0 & 0 & -2(k_c+k_s)-\lambda \end{vmatrix} = 0$$

Solution of the above gives the eigenvalues:

$$\lambda_1 = -3k_s/2 - 5k_c/2 + (1/2)(5k_c^2 + 10k_ck_s + 9k_s2)^{1/2}$$

$$\lambda_2 = -7k_s/2 - 5k_c/2 + (1/2)(5k_c^2 + 2k_ck_s + k_s^2)^{1/2}$$

$$\lambda_3 = 0$$

$$\lambda_4 = -3k_s/2 - 5k_c/2 - (1/2)(5k_c^2 + 10k_ck_s + 9k_s^2)^{1/2}$$

$$\lambda_5 = -7k_s/2 - 5k_c/2 - (1/2)(5k_c^2 + 2k_ck_s + k_s^2)^{1/2}$$

The last three eigenvalues correspond to eigenintensities that are invariant with time. Numerical and algebraic solutions of the eigenvalue problem for λ_1 and λ_2 and the corresponding eigenintensities $Q1$ and $Q2$ were obtained using the program MAPLE operating on a SUN/3 workstation. Evaluation of the $t = \infty$ values of experimental intensities (including the $Q2$ eigenintensity) were performed with the program CONINFIN[27] (available through Project Seraphim). Linear regression analyses were carried out with Lotus 1-2-3.

Supplementary Material Available: Tables giving raw and normalized intensity versus time data, derivation of eigenintensities $Q1$ and $Q2$, first-order rate constants k_c and k_s, and Eyring analysis of rate constants k_c and k_s (8 pages). Ordering information is given on any masthead page.

(26) (a) Dewar, M. J. S.; Thiel, W. *J. Am. Chem. Soc.* **1977**, *99*, 4899. (b) *QCPE*, **1984**, No. 455 (MOPAC).

(27) Houser, J. J. *J. Chem. Educ.* **1982**, *59*, 776.

Oxygen-17 Nuclear Magnetic Resonance Spectroscopic Studies of Carbonmonoxy Hemoproteins

Hee Cheon Lee and Eric Oldfield*

Contribution from the School of Chemical Sciences, University of Illinois at Urbana-Champaign, 505 South Mathews Avenue, Urbana, Illinois 61801. *Received June 22, 1988*

Abstract: We have obtained surprisingly narrow ^{17}O nuclear magnetic resonance (NMR) spectra at 8.45 and 11.7 T (corresponding to ^{17}O frequencies of 48.8 and 67.8 MHz) from $C^{17}O$ ligands bound to aqueous ferrous myoglobin from *Physeter catodon* (sperm whale MbCO), from adult human ferrous hemoglobin (HbCO A), and from ferrous hemoglobin from *Oryctolagus cuniculus* (rabbit HbCO). The ^{17}O NMR signals from these hemoproteins are not only narrower than anticipated, but in the case of sperm whale MbCO the line shape is distinctly non-Lorentzian. We have thus used the dispersion versus absorption (DISPA) plot method to investigate the origin of these unusual line widths and line shapes and demonstrate that they originate from the multiexponential nature of quadrupolar relaxation outside of the "extreme-narrowing" limit ($\omega_0\tau_c > 1$). We find from the DISPA analysis and from spin-lattice relaxation time (T_1) measurements that the ^{17}O nuclear quadrupole coupling constant (QCC) for sperm whale MbCO is 0.95 MHz, and the rotational correlation time, τ_c, is 14 ns (at $\omega_0\tau_c = 5.8$). This indicates a rigid heme-CO unit in sperm whale MbCO. Applying the same type of analysis to human HbCO yields ^{17}O QCC values of 0.9 MHz and τ_c of 23 ns (at $\omega_0\tau_c = 10$). In all cases, our results are consistent with an ^{17}O chemical shift anisotropy ($\sigma_\parallel - \sigma_\perp$) value of about 800 ppm for the CO ligand. These results are important for several reasons: first, they represent the first observation of high-resolution ^{17}O NMR spectra of the CO ligands in metalloproteins. Second, they represent the first experimental demonstration of multiexponential relaxation of a spin $I = {}^5/_2$ nucleus and its complete analysis with relaxation theory. Third, our results on sperm whale MbCO, taken together with ^{13}C NMR relaxation data, indicate little "internal motion" of the heme-CO group in this system. Our results also demonstrate a linear relationship between the ^{17}O NMR chemical shift and ν_{CO}, the infrared stretching frequency of the CO ligand, and between the ^{17}O chemical shift and the CO binding affinity of the protein. In addition, the ^{17}O NMR results are also in good agreement with previous time-differential perturbed γ-ray angular correlation (PAC) results on [^{111}In]myglobin and -hemoglobin (Marshall, A. G.; Lee, K. M.; Martin, P. W. *J. Am. Chem. Soc.* **1980**, *102*, 1460), and some molecular interpretations of the NMR and PAC results are offered.

In the absence of functional interactions, when ligand binding sites may be assumed to be equivalent and independent, different hemoproteins show large differences in their affinity for, and rates of reaction with, the same ligand, even though the overall arrangements of the polypeptide chains are similar.[1] Available evidence implies that the reactivity of the heme in hemoproteins is primarily controlled by local effects due to neighboring groups

(1) Antonini, E.; Brunori, M. In *Hemoglobin and Myoglobin in Their Reactions with Ligands*; American Elsevier: New York, 1971.

0002-7863/89/1511-1584$01.50/0

on the polypeptide chain. For example, structural analyses reveal that the Fe–CO unit in carbonmonoxymyoglobin (MbCO) or carbonmonoxyhemoglobin (HbCO) is bent and/or tilted with respect to the porphyrin ring, due to interactions with the distal amino acid residues,[2-5] whereas in heme model compounds, free from protein effects, the Fe–CO unit is linear and normal to the heme plane.[6] Thus it has been proposed[7,8] that one of the primary functions of the amino acids on the distal side of the heme is to provide a sterically crowded environment, which would lower CO affinity by distortion of the preferred, linear, Fe–CO geometry. However, direct and unequivocal evidence concerning all of the factors that affect heme reactivity are still lacking.

Since the oxygen atom of CO bound to hemoproteins is in close contact with the distal residues, ^{17}O NMR appears to be a potentially useful probe for investigating local structural effects on ligand binding affinities of hemoproteins in solution. Surprisingly, however, no attempts appear to have been made to use ^{17}O NMR as a probe of such interactions, presumably because ^{17}O NMR of macromolecules might be expected to give very broad signals because of rapid quadrupolar relaxation of the ^{17}O nucleus due to slow molecular tumbling.

However, NMR of quadrupolar nuclei in macromolecules not only gives, in general, rather broad signals but also exhibits rather complicated relaxation behavior when the rotational correlation time, τ_c, is not short compared with the Larmor frequency, ω_0. Indeed, it has been shown[9-12] that decay of both the transverse *and* the longitudinal magnetization of quadrupolar nuclei in the slow-motion limit ($\omega_0\tau_c \geq 1$) is not a simple exponential but a sum of $(I + {}^1/_2)$ exponentials for half-integer spin nuclei. For such nuclei, detailed line shape and/or relaxation studies can permit determination of *both* the nuclear quadrupole coupling constant (QCC) and the rotational correlation time, τ_c. Moreover, it is found that one of the exponentials is in fact rather long, yielding *narrow line spectra*, for $\omega_0\tau_c > 1$ (see below).

Whereas multiexponential behavior for spin $I = {}^3/_2$ nuclei has been frequently observed,[13-16] so far no clear-cut example of multiexponential relaxation of spin $I = {}^5/_2$ or $I = {}^7/_2$ nuclei has been reported, even though the differences in the *apparent* (due to chemical exchange) longitudinal relaxation time, T_1, and transverse relaxation time, T_2, have been encountered for $I = {}^5/_2$[17] and $I = {}^7/_2$ nuclei.[18] We report herein our observation of multiexponential ^{17}O NMR signals from MbCO and HbCO and also report the QCC and τ_c of CO bound to several hemoproteins as determined from line shape and relaxation data by using a DISPA (dispersion versus absorption) analysis.[19] This is, to the best of our knowledge, the first experimental demonstration of multiexponential relaxation of spin $I = {}^5/_2$ nuclei, and its complete analysis with relaxation theory, in systems that are not complicated by the effects of chemical exchange, which has been a controversial topic in this area.[15,16]

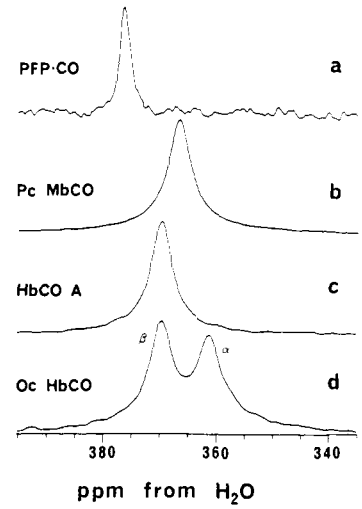

Figure 1. ^{17}O NMR spectra of ^{17}O-labeled carbonmonoxy hemoproteins and a model compound at 11.7 T and 29 °C: (a) 1 mM CO-picket fence porphyrin in benzene (22 804 scans, 102-ms recycle time, 40-μs 90° pulse width, and 50-Hz line broadening); (b) 12 mM sperm whale MbCO in 50 mM phosphate buffer, pH = 7.0 (212 660 scans, 62-ms recycle time, 38-μs 90° and 80-μs 180° pulse widths, and 100-Hz line broadening); (c) 2.5 mM (in tetramer) human HbCO in 50 mM phosphate buffer, pH = 7.0 (400 000 scans, 102-ms recycle time, 38-μs 90° and 80-μs 180° pulse widths, and 100-Hz line broadening); (d) 2.5 mM (in tetramer) rabbit HbCO in 50 mM phosphate buffer, pH = 7.0 (280 000 scans, 202-ms recycle time, 37-μs 90° and 78-μs 180° pulse widths, and 100-Hz line broadening).

Of particular importance, we believe, is our observation that the ^{17}O line widths of CO ligands bound to large macromolecules are much narrower than might be expected based on a simple extrapolation of results obtained in the extreme-narrowing case.[20] For example, we demonstrated previously that the ^{17}O NMR line widths for $^{17}O_2$ in Vaska's compound ($\tau_c \sim 100$ ps, $e^2qQ/h \sim 16.5$ MHz) were ~9 kHz. A straightforward, but incorrect, calculation of the line width expected for HbCO ($\tau_c \sim 30$ ns, $e^2qQ/h \sim 1.0$ MHz) then yields, based on the differences in τ_c and e^2qQ/h, $W \sim 10$ kHz, a very large value. Experimentally, however, we find an apparent line width of $W \sim 200$ Hz, 50 times smaller, due to multiexponential relaxation and the fact that $\omega_0\tau_c > 1$. This observation of spectral line widths nearly 2 orders of magnitude narrower than might have been anticipated from a simple $\tau(QCC)^2$ extrapolation from previous model compound studies ($\omega\tau_c \ll 1$) means that a wide new area of NMR studies of CO ligand binding to proteins is now feasible with conventional NMR instrumentation. In this paper we show that both τ_c and QCC information for the CO ligand, in addition to its chemical shift and chemical shift anisotropy, may be obtained in a fairly unambiguous manner.

Experimental Section

Sperm whale (*Physeter catodon* (Pc)) myoglobin (Mb), human adult hemoglobin (Hb), and rabbit (*Oryctolagus cuniculus* (Oc)) Hb were purchased from Sigma Chemical Co. (St. Louis, MO). C^{17}O (36% ^{17}O) was obtained from ICON Services, Inc. (Summit, NJ). The "picket fence porphyrin", Fe($\alpha,\alpha,\alpha,\alpha$-$T_{piv}$PP)(1-MeIm)CO, was prepared by the method described in the literature[21] from free ($\alpha,\alpha,\alpha,\alpha$-$T_{piv}$PP), purchased from Mid Century Chemicals (Posen, IL). For the preparation of MbCO, ferric Mb was reduced anaerobically with sodium dithionite in a 50 mM phosphate buffer at pH = 7.0 and then carbonylated. Small molecules were removed on a Sephadex G-25 (medium) column. Protein

(2) Baldwin, J. M. *J. Mol. Biol.* **1980**, *136*, 103.
(3) Heidner, E. J.; Ladner, R. C.; Perutz, M. F. *J. Mol. Biol.* **1976**, *104*, 707.
(4) Norvell, J. C.; Nunes, A. C.; Schoenborn, B. P. *Science* **1975**, *190*, 568.
(5) Bianconi, A.; Congiu-Castellano, A.; Durham, P. J.; Hasnain, S. S.; Phillips, S. *Nature* **1985**, *318*, 685.
(6) Peng, S. M.; Ibers, J. A. *J. Am. Chem. Soc.* **1976**, *98*, 8032.
(7) Collman, J. P.; Brauman, J. I.; Halbert, T. R.; Suslick, K. S. *Proc. Natl. Acad. Sci. U.S.A.* **1976**, *73*, 3333.
(8) Caughey, W. S. *Ann. N.Y. Acad. Sci.* **1970**, *174*, 148.
(9) Bull, T. E.; Forsén, S.; Turner, D. L. *J. Chem. Phys.* **1979**, *70*, 3106.
(10) Hubbard, P. S. *J. Chem. Phys.* **1970**, *53*, 985.
(11) Reuben, J.; Luz, Z. *J. Phys. Chem.* **1976**, *80*, 1357.
(12) Westlund, P.; Wennerström, H. *J. Magn. Reson.* **1982**, *50*, 451.
(13) Gustavsson, H.; Lindman, B.; Bull, T. *J. Am. Chem. Soc.* **1978**, *100*, 4655.
(14) Delville, A.; Detellier, C.; Laszlo, P. *J. Magn. Reson.* **1979**, *34*, 301.
(15) Marshall, A. G.; Wang, T.-C. L.; Cottrell, C. E.; Werbelow, L. G. *J. Am. Chem. Soc.* **1982**, *104*, 7665.
(16) Lerner, L.; Torchia, D. A. *J. Am. Chem. Soc.* **1986**, *108*, 4264.
(17) Petersheim, M.; Miner, V. W.; Gerlt, J. A.; Prestegard, J. H. *J. Am. Chem. Soc.* **1983**, *105*, 6357.
(18) Andersson, T.; Drakenberg, T.; Forsén, S.; Thulin, E.; Swärd, M. *J. Am. Chem. Soc.* **1982**, *104*, 576.
(19) Marshall, A. G. In *Fourier, Hadamard, and Hilbert Transforms in Chemistry*; Marshall, A. G., Ed.; Plenum Press: New York, 1982; pp 99–123.
(20) Lee, H. C.; Oldfield, E. *J. Magn. Reson.* **1986**, *69*, 367.
(21) Collman, J. P.; Gagne, R. R.; Reed, C. A.; Halbert, T. R.; Lang, G.; Robinson, W. T. *J. Am. Chem. Soc.* **1975**, *97*, 1427.

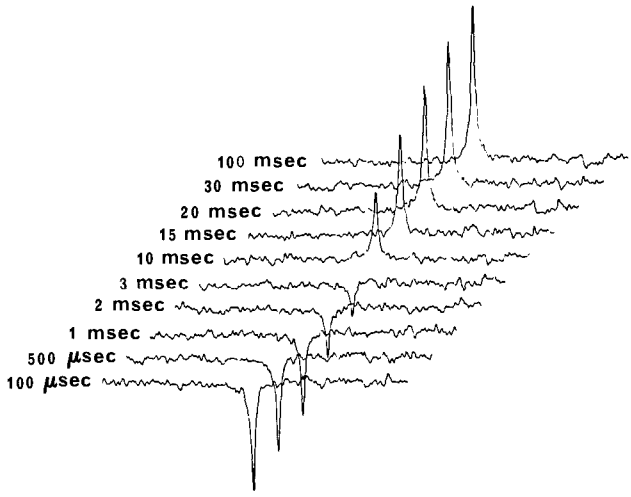

Figure 2. Partially relaxed Fourier transform inversion–recovery (180°–τ–90°) data set for sperm whale MbC^{17}O at 11.7 T (5000 scans, 72-ms recycle time, 38-μs 90° and 81-μs 180° pulse widths, and 200-Hz line broadening). The τ values are given on the figure.

Table I. Spectroscopic Properties and Ligand Binding Affinities of ^{17}O-Labeled Carbonmonoxy Hemoproteins and a Model System

sample	chem shift (δ_i, ppm)[a]	T_1, ms	$P_{1/2}$(CO),[b] Torr	ν_{CO},[c] cm^{-1}
picket fence porphyrin-C^{17}O	376	4	irreversible	1967
sperm whale MbC^{17}O	366.5	9	0.018	1944
human HbC^{17}O α,β chains	369	16	0.004[d]	1951
rabbit HbC^{17}O β chain	369	19		1951
rabbit HbC^{17}O α chain	361	32		1928

[a] Chemical shift in ppm from internal $H_2{}^{17}O$ at 29 °C. [b] Reference 7. [c] References 7 and 25. [d] $P_{1/2}$(CO) for the binding of the fourth CO.

solutions were then concentrated in a Model 8050 ultrafiltration cell (Amicon Corp., Danvers, MA) equipped with a suitable Diaflo membrane. The pH was measured at room temperature with a Radiometer PHM 62 meter (Cleveland, OH), and the final pH was adjusted with 1 M NaOH or 1 M HCl. Similar procedures were used for the preparations of human HbCO and rabbit HbCO.

^{17}O NMR spectra were obtained at 8.45 and 11.7 T (corresponding to ^{17}O resonance frequencies of 48.8 and 67.8 MHz, respectively) on "home-built" spectrometers, which consist of 8.45-T 89-mm-bore or 11.7-T 52-mm-bore superconducting solenoids (Oxford Instruments, Osney Mead, U.K.), Nicolet (Madison, WI) Model 1280 data acquisition systems, Amplifier Research (Souderton, PA) Model 200L amplifiers for radio frequency pulse generation, and either a 10- or a 20-mm multinuclear solution NMR probe (Cryomagnet Systems, Indianapolis, IN). All the spectra were recorded from static samples, using a spin–echo pulse sequence (90°–τ–180°–τ–acquire) with 16 step phase cycling.[22] The 90° pulse widths were between 35 and 40 μs, and typical recycle times of between 100 and 300 ms were employed. Chemical shifts were referenced to internal natural-abundance $H_2{}^{17}O$ at 0 ppm, using the convention that high-frequency, low-field, paramagnetic, deshielded values are positive (IUPAC δ scale). All experiments were performed at 29 ± 2 °C and at pH = 7.0.

^{13}C NMR spectra were obtained at 8.45 T (corresponding to a ^{13}C resonance frequency of 90.5 MHz) on the same "home-built" spectrometer as described above. Spin–lattice relaxation times (T_1) were measured on the same sample as used for ^{17}O NMR and at the same probe temperature, using the inversion–recovery pulse sequence, together with 4-W WALTZ-16 proton decoupling. The 90° pulse width was 44 μs.

Results and Discussion

Contrary to our initial expectation, we have observed quite narrow ^{17}O NMR signals from sperm whale MbC^{17}O, human HbC^{17}O, and rabbit HbC^{17}O. Figure 1 shows the ^{17}O NMR spectra of these hemoproteins, together with that of a model compound, CO-picket fence porphyrin. The signal-to-noise ratios are adequate to permit meaningful inversion–recovery T_1 measurements, and we show in Figure 2 representative partially relaxed Fourier transform ^{17}O NMR spectra for sperm whale MbC^{17}O. Table I contains a compilation of all of the ^{17}O NMR chemical shift and T_1 data, together with affinity constant data[7] and infrared CO stretching frequencies.

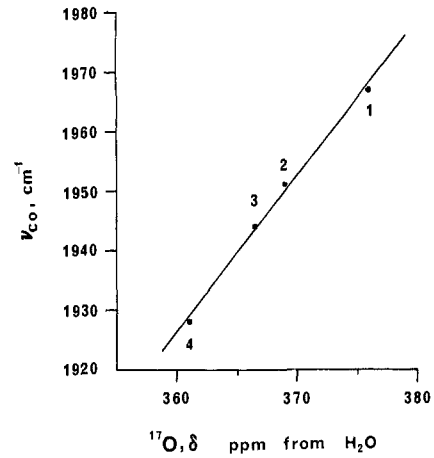

Figure 3. Plot of the ^{17}O NMR chemical shifts versus infrared $^{12}C^{16}O$ stretching frequencies: (1) CO-picket fence porphyrin; (2) human Hb α and β chains and rabbit Hb β chain; (3) sperm whale MbCO; (4) rabbit Hb α chains.

A single ^{17}O NMR signal is observed from sperm whale MbCO (Figure 1b), while two signals are observed from rabbit HbCO (one for each type of chain) (Figure 1d), as expected. However, only a single signal is observed from human HbCO, in contrast to the observation[23] that the ^{13}C NMR spectrum of HbCO A exhibits two well-resolved signals. This highlights the only apparent drawback of ^{17}O NMR of C^{17}O-labeled proteins—that resolution of ^{17}O NMR is less than that of ^{13}C NMR, due primarily to increased ^{17}O line widths.

In order to check on the origins of our ^{17}O NMR resonances, we have titrated the sperm whale MbCO sample with $K_3Fe(CN)_6$ to remove the possibility that the broad signal might originate from mobile, free CO "trapped" in the protein matrix. The broad signals gradually and stoichiometrically disappear in proportion to the amount of $K_3Fe(CN)_6$ added, which confirms that the broad signal observed represents CO bound to Fe(II) of the hemoprotein. In rabbit HbCO, we assign the peak at 369 ppm to the β chains and the peak at 361 ppm to the α chains. These specific assignments are based on the observation by previous workers[23-25] that the β chains resemble the α and β chains of human Hb, while the α chains may be preferentially oxidized with oxidants such as $K_3Fe(CN)_6$. In our oxidation experiments (data not shown) the peak at 361 ppm disappears first when fractional equivalents of $K_3Fe(CN_6)$ are added to the protein solution. We have also titrated the ^{17}O NMR spectra of all the hemoproteins studied with 1 M HCl and 1 M NaOH and observe no pH dependence of the ^{17}O chemical shifts between pH 6 and pH 11 (data not shown).

The results of Table I suggest a correlation exists between infrared CO stretching frequencies and ^{17}O NMR chemical shifts for bound CO's, both in the model compound and in the hemoproteins. A plot of the ^{17}O NMR chemical shifts versus (average) IR stretching frequencies is given in Figure 3 and shows an excellent linear relationship, as has been observed previously for transition-metal carbonyls.[26,27] The ^{17}O NMR chemical shift also appears to correlate with previously measured CO affinity constants,[7] although the data base here is extremely limited. Nevertheless, it does appear in the picket fence porphyrin, which

(22) Kunwar, A. C.; Turner, G. L.; Oldfield, E. *J. Magn. Reson.* **1986**, *69*, 124.

(23) Moon, R. B.; Richards, J. H. *Biochemistry* **1974**, *13*, 3437.
(24) Matwiyoff, N. A.; Vergamini, P. J.; Needham, T. E.; Gregg, C. T.; Volpe, J. A.; Caughey, W. S. *J. Am. Chem. Soc.* **1973**, *95*, 4429.
(25) Satterlee, J. D.; Teintze, M.; Richards, J. H. *Biochemistry* **1978**, *17*, 1456.
(26) Gray, G. M.; Kraihanzel, C. S. *J. Organomet. Chem.* **1983**, *241*, 201.
(27) Cozak, D.; Butler, I. S.; Hickey, J. P.; Todd, L. J. *J. Magn. Reson.* **1979**, *33*, 149.

Table II. Experimental and Theoretical Oxygen-17 NMR Relaxation Parameters for MbC^{17}O

	expt			theory[a]		
	T_1, ms	line width,[b] Hz	area (t = 0),[c] %	T_1, ms	line width, Hz	area (t = 0), %
narrow component	9	196 (96)	44 (60)	9	95	36
broad component	NM[d]	910 (810)	56 (40)	NM[d]	812	64

[a] Relaxation parameters for pure quadrupolar interaction.[9] $\omega_0\tau_c = 5.8$, $\omega_0 = 4.26 \times 10^8$ s^{-1}, and QCC = 0.95 MHz. [b] The values in parentheses represent the quadrupolar contribution to the line width, as discussed in the text. [c] The values in parentheses are relative areas at t = 303 μs. [d] Not measurable.

is free from steric effects due to protein side chains (although, of course, other important steric effects are present), that irreversible CO binding correlates with the most downfield-shifted ^{17}O resonance signal, while, on the other hand, the rabbit Hb α chain, which is the most unstable,[25] yields the most upfield-shifted signal. Such differences in ^{17}O NMR chemical shift behavior may be attributable to the degree of distal amino acid interaction with the heme-bound CO.

The ^{17}O NMR signals from MbCO and HbCO not only are narrower than might have been anticipated but are also non-Lorentzian in shape, as can be seen in Figure 1. Furthermore, the measured T_1 is much greater than the T_2 deduced from the *apparent* line width. This suggests that the non-Lorentzian ^{17}O NMR signals originate from quadrupolar relaxation in the slow-motion limit ($\omega_0\tau_c > 1$).

For an $I = {}^5/_2$ nucleus, it has been shown previously[10] that the decay of both longitudinal and transverse magnetization is a weighted sum of three exponentials in the slow-motion limit and can be written as

$$\Delta M_1(t) = \Delta M_1(0)\sum_{i=1}^{3} C_{1,i} \exp(-R_{1,i}t) \quad (1)$$

$$M_2(t) = M_2(0)\sum_{i=1}^{3} C_{2,i} \exp(-R_{2,i}t) \quad (2)$$

where

$$\sum_{i=1}^{3} C_{1,i} = \sum_{i=1}^{3} C_{2,i} = 1$$

and the subscripts 1 and 2 denote longitudinal and transverse relaxation, respectively. Since the preexponential factors, as well as the exponential factors, in eq 1 and 2 depend on parameters such as ω_0, τ_c, etc., it is not possible to obtain analytical solutions of the relaxation equations, and they have to be solved numerically for each $\omega_0\tau_c$ value. Such numerical calculations for $I = {}^5/_2$ nuclei have been performed by Bull et al.[9]

The decay of the longitudinal magnetization, however, can be approximated by a single exponential for correlation times such that $\omega_0\tau_c \leq 10$, since $C_{11} > 0.93$ for $\omega_0\tau_c \leq 10$. For such a "nearly exponential" relaxation, the longitudinal relaxation rate can be written[18,28] as

$$R_1 = \frac{1}{T_1} = \frac{3\pi^2}{50}\,\frac{2I+3}{I^2(2I-1)}\left(\frac{e^2qQ}{h}\right)^2\left[\frac{\tau_c}{1+\omega_0^2\tau_c^2} + \frac{4\tau_c}{1+4\omega_0^2\tau_c^2}\right] \quad (3)$$

where the symbols have their usual meanings. Thus we can obtain well-defined T_1 values using inversion–recovery techniques, even though the line shapes are still non-Lorentzian.

We have performed inversion–recovery T_1 measurements for sperm whale MbCO at two different magnetic field strengths in order to clarify relaxation mechanisms and have obtained T_1 values of 9 ms at 11.7 T and 5.3 ms at 8.45 T. Since the experimental T_1 ratio of 1.7 at the two fields is very close to the theoretical value of 1.9 (from eq 3 when $\omega_0\tau_c > 1$), we can thus confirm that the quadrupolar interaction is the dominant spin–lattice relaxation mechanism for C^{17}O in aqueous MbC^{17}O solutions.

(28) Halle, B.; Wennerström, H. *J. Magn. Reson.* **1981**, *44*, 89.

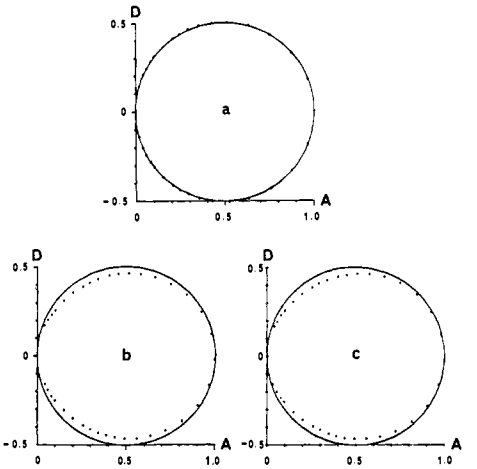

Figure 4. DISPA plots for sperm whale MbC^{17}O in H_2O: (a) experimental DISPA plot for the $H_2{}^{17}O$ signal in the MbC^{17}O sample; (b) experimental DISPA plot for sperm whale MbC^{17}O; (c) simulated DISPA plot for sperm whale MbC^{17}O. The experimental DISPA plot in (b) was constructed from the spectrum in Figure 1b, which had been Fourier transformed at t = 303 μs from t = 0.

In order to further investigate the origins of the observed line shapes of the ^{17}O NMR signals from MbCO and HbCO, we have used the dispersion versus absorption (DISPA) method to monitor slight deviations from Lorentzian behavior. Figure 4a shows the experimental DISPA plot for the $H_2{}^{17}O$ signal in our MbCO sample. The circularity of the DISPA plot indicates a near-perfect Lorentzian line shape. Thus any deviations from the DISPA reference circle (diameter equal to maximum absorption peak height) for other signals in the same sample must almost certainly reflect the intrinsic properties of the line shape rather than any experimental artifacts.

Figure 4b shows the experimental DISPA plot for the C^{17}O ligands in sperm whale MbC^{17}O. According to Marshall's analysis,[19] there is only one possible mechanism that can displace the DISPA plot inward and to the left of its reference circle with a magnitude as large as in Figure 4b. That is the case of a superposition of several Lorentzians having the same resonance frequency but different line widths, as shown for example in Figure 5. The experimental DISPA plot can be simulated by varying the areas and line widths of each component independently, but keeping the same resonance frequency. We have found that an excellent DISPA simulation can be obtained by using two components, rather than three, as shown in Figure 4c, and the line widths and relative areas of each component for MbCO are listed in Table II. Since the experimental DISPA plot was constructed from a spectrum that had been Fourier transformed at t = 303 μs from t = 0 (due to the instrumental dead time, finite 180° pulse duration, and the delays (τ) between and after pulses), the relative areas at t = 0 (the relative amplitude $C_{2,i}$ in eq 2) have been extrapolated from those at t = 303 μs. Attempts at simulating the DISPA plot with three components did not yield any improvement. We have also simulated the ^{17}O NMR spectrum of MbC^{17}O independently, using two Lorentzian peaks, as shown in Figure 5. The line widths and relative areas of each component are in excellent agreement with those obtained from the DISPA plot. Note, however, that relaxation theory[10] and numerical calculations[9] for the transverse relaxation rates of spin $I = {}^5/_2$

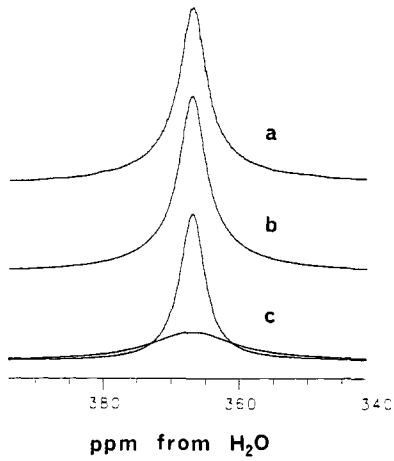

Figure 5. Line shapes for sperm whale MbCO at 11.7 T: (a) experimental ^{17}O NMR spectral line shape from Figure 1b; (b) simulated line shape; (c) Lorentzian peaks used in simulation in (b) having line widths of 196 Hz for the narrow component and 910 Hz for the broad component. Area ratio = 60/40 (narrow/broad). The experimental spectrum was obtained by Fourier transforming the FID at t = 303 μs from t = 0.

nuclei do predict three components, a narrow one, an intermediate one, and a broad one. The line width of the narrow component decreases as τ_c increases in the slow-motion limit, while those of the intermediate and broad components increase. However, Lerner and Torchia have shown[16] that, as expected, the line width of the narrow component does not necessarily decrease as τ_c increases if the chemical shift anisotropy (CSA) is large. We have also observed such behavior from temperature and magnetic field strength dependence studies of the ^{17}O NMR spectra of our MbC^{17}O samples (data not shown). This suggests that the CSA contribution to the line width is not small. Indeed, solid-state "magic-angle" sample-spinning ^{17}O NMR studies of CO-picket fence porphyrin show[29] that the ^{17}O CSA of CO bound to Fe(II) is very large (ca. 800 ppm), while the ^{17}O QCC is very small (ca. 1 MHz). We thus assign the narrow and broad components obtained from the DISPA plot to the narrow and intermediate ones predicted by relaxation theory. The third and broadest component predicted is presumably not observable because it relaxes too rapidly.

We now have three experimental relaxation parameters: T_1 of the narrow component, and the line widths of both the narrow and broad components, which are sufficient to determine the two unknowns, the ^{17}O QCC of CO bound to Mb and its τ_c. However, we have found that the three experimental parameters do not match simultaneously with the theoretical ones at any combination of QCC and τ_c, since there are additional nonquadrupolar interactions, such as the chemical shift anisotropy and various instrumental contributions to the line width, which need to be taken into consideration. We can investigate these factors as follows. First, we can estimate the CSA contribution to the line width. The relaxation rates for the CSA mechanism are given by

$$\frac{1}{T_1} = \frac{1}{15}\gamma^2 H_0^2(\sigma_\parallel - \delta_\perp)^2\left\{\frac{2\tau_c}{1+\omega^2\tau_c^2}\right\} \quad (4)$$

$$\frac{1}{T_2} = \frac{1}{90}\gamma^2 H_0^2(\sigma_\parallel - \sigma_\perp)^2\left\{\frac{6\tau_c}{1+\omega^2\tau_c^2} + 8\tau_c\right\} \quad (5)$$

where the symbols have their usual meanings. For $\tau_c \approx 14$ ns and $|\sigma_\parallel - \sigma_\perp| = 800$ ppm (the CO-picket fence porphyrin value[29]) we find a CSA contribution to the line width of ~50 Hz. The CSA contribution to T_1 is negligible (170 ms). We have also measured T_1 of the water in the MbCO sample and obtain T_1 = 4.9 ms. Since the measured line width of the water signal is 95 Hz, this

(29) Lee, H. C.; Oldfield, E., unpublished results.

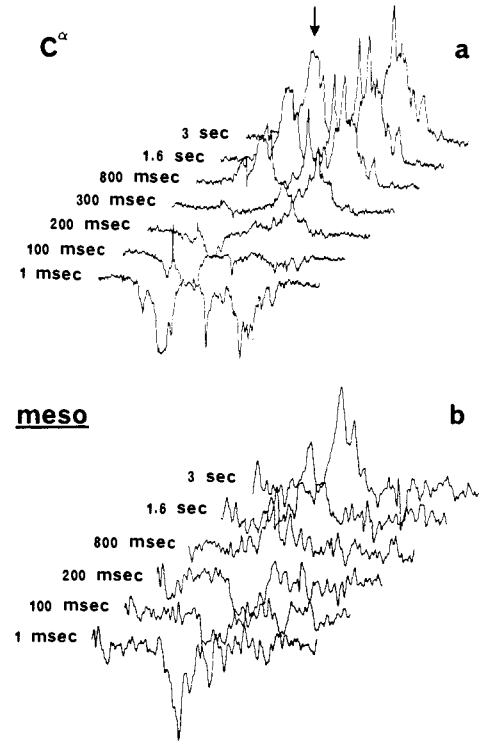

Figure 6. Partially relaxed Fourier transform inversion–recovery (180°–τ–90°) data sets for the polypeptide C^α and heme meso carbons in sperm whale MbCO from the same sample as used for ^{17}O NMR in Figure 1b. The τ values are given on the figure. (a) C^α carbons (500 scans, 3.3-s recycle time, 44-μs 90° and 90-μs 180° pulse widths, 20-Hz line broadening, 4-W WALTZ-16 ^1H decoupling); (b) heme meso carbons (3000 scans, 3.3-s recycle time, 44-μs 90° and 90-μs 180° pulse widths, 30-Hz line broadening, 4-W WALTZ-16 ^1H decoupling).

indicates a magnetic inhomogeneity contribution of ~30 Hz, with the assumption that $T_1 = T_2$ for water. We note that the assumption of $T_1 = T_2$ is not valid for pure water at neutral pH, due to ^1H–^{17}O scalar coupling effects.[30] However, such line broadening appears to be minimal for our concentrated protein solutions, as indicated by the near-perfect Lorentzian line shape of the $H_2{}^{17}O$ signal in the protein sample, presumably due to a significantly decreased proton lifetime (caused either by buffer[31] or solvent-accessible functional groups in the protein[32]). Thus our results indicate a nonquadrupolar contribution to the ^{17}O line width of CO[17] in MbC^{17}O of about 80 Hz.

What we find experimentally (Table II) is that a 100-Hz correction, rather than 80 Hz, is required in order to obtain a unique solution for τ_c and QCC, which predicts all three measured parameters—the T_1 and line widths of both DISPA components. Although the correction is a substantial fraction of the experimentally observed line width, we believe it is clearly within typical experimental error (on both T_1 and T_2), the unaccounted for 20-Hz line width being only 10% of the measured width of the narrow component, and could easily be due to a slightly larger CSA alone in MbCO, which is quite possible in view of increased π backbonding, due to the bend and/or tilted Fe–CO unit.[33] With this minor caveat then, we obtain a unique solution of a QCC of 0.95 MHz and τ_c = 14 ns for MbC^{17}O (at $\omega_0\tau_c$ = 5.8). The ^{17}O QCC obtained is comparable with those observed in mononuclear transition-metal carbonyls (ca. 1 MHz).[29,34] Furthermore, the τ_c value of 14 ns is very close to the values of 13 and 12 ns obtained from ^{13}C (T_1) measurements of the C^α carbon in the protein backbone and the (meso) methine carbon in the heme group,

(30) Meiboom, S. *J. Chem. Phys.* **1961**, *34*, 375.
(31) Noack, F. *Prog. NMR Spectrosc.* **1987**, *18*, 171.
(32) Rose, K. D.; Bryant, R. G. *J. Am. Chem. Soc.* **1980**, *102*, 21.
(33) Li, X. Y.; Spiro, T. G. *J. Am. Chem. Soc.* **1988**, *110*, 6024.
(34) Oldfield, E.; Keniry, M. A.; Shinoda, S.; Schramm, S.; Brown, T. L.; Gutowsky, H. S. *J. Chem. Soc., Chem. Commun.* **1985**, 791.

Table III. Experimental and Theoretical Oxygen-17 NMR Relaxation Parameters for Human HbC^{17}O

	expt			theory[a]		
	T_1, ms	line width,[b] Hz	area (t = 0), %	T_1, ms	line width, Hz	area (t = 0), %
narrow component	16	196 (56)	44	16	50	35
broad component	NM[c]	1200 (1060)	56	NM[c]	1067	65

[a] Relaxation parameters for pure quadrupolar interaction.[9] $\omega_0\tau_c = 10$, $\omega_0 = 4.26 \times 10^8$ s^{-1}, and QCC = 0.9 MHz. [b] The values in parentheses represent the purely quadrupolar contributions to the line width, as discussed in the text. [c] Not measurable.

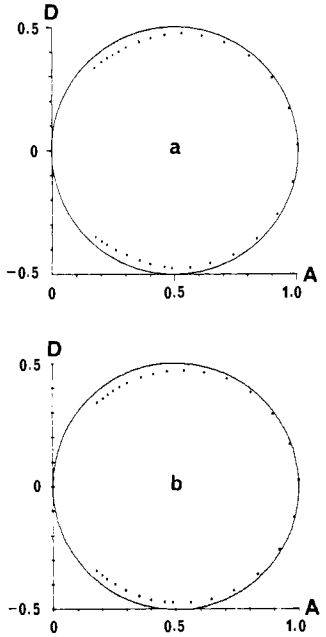

Figure 7. Experimental and simulated DISPA plots for human HbC^{17}O: (a) experimental DISPA plot; (b) simulated DISPA plot. The DISPA plot in (a) was constructed from the spectrum in Figure 1c, which had been Fourier transformed at t = 303 μs from t = 0.

respectively, as shown in Figure 6, determinations that were made on the same sample as used for ^{17}O NMR and at the same probe temperature. These τ_c values are to be compared with our previous result[35] of τ_c = 22 ns for ^{57}Fe in MbCO, obtained at a slightly higher concentration and lower temperature. The close similarities of τ_c values for the peptide C$^\alpha$, heme meso carbon, and heme CO oxygen clearly imply little internal motion of the heme, or its CO ligand, or at least that all motions are likely very small amplitude librations.

We have also applied a similar line shape analysis to the ^{17}O NMR spectrum of human HbCO. The experimental and simulated DISPA plots for HbCO are shown in Figure 7, and the line widths and the relative areas of the two Lorentzian peaks used are listed in Table III. While there could be small chemical shift differences between the α and β chains of human HbCO, several factors prompted us to use the same procedures as with MbCO. First, we did not see any indication of such a shift difference. Second, Marshall et al.[36] have shown that a distribution in peak position not only displaces the DISPA plot outward from its reference circle but also dominates over a distribution in line width in determining the DISPA displacement. However, we do not observe any evidence of such a distribution in peak position from the experimental DISPA plot for HbCO. Third, the *apparent* line width of the ^{17}O NMR signal from human HbCO is almost the same as (or even less than) that of the β chain of rabbit HbCO (which gives approximately the same ^{17}O NMR chemical shift as human HbCO). Taken together, we conclude that the oxygen environments of CO bound to both the α and β chains of human HbCO are very similar and that any differences in ^{17}O NMR chemical shift between them are unmeasurable.

The experimental and theoretical relaxation parameters determined for HbCO A are listed in Table III and correspond to a QCC of 0.9 MHz and τ_c = 23 ns (at $\omega_0\tau_c$ = 10). The line width subtraction of 140 Hz is large (for the narrow component) but is not unexpected, since Hb is 4 times larger than Mb, and the CSA contribution to the line width becomes larger as τ_c increases. Indeed, a CSA contribution of 80 Hz is obtained at τ_c = 23 ns (from eq 5), using the picket fence porphyrin CSA of 800 ppm, and this together with a 30-Hz magnetic inhomogeneity contribution accounts for almost 80% of the line width correction. The resultant QCC and τ_c values are again in excellent agreement with those derived from other studies.[29,34,37,38]

Rabbit HbCO displays two well-resolved ^{17}O NMR signals for the α and β chains (Figure 1d). The signal from the β chain appears slightly downfield from that of human HbCO, whereas the signal from the α chain is shifted considerably upfield. These shifts are opposite to those found with ^{13}C NMR,[23] a not unusual occurrence with (other) substituted transition-metal carbonyls.

Unfortunately, the presence of two well-resolved peaks imposes some difficulties in applying the DISPA analysis, since now eight parameters have to be varied independently instead of four. What is clear, however, is that there are large structural differences between the α and β chains, as reflected in the C^{17}O T_1 values of 32 and 19 ms, respectively. If we assume a QCC value of 0.95 MHz, as with HbCO A, then use of eq 3 yields τ_c values of 51 and 30 ns, respectively, for the α and β CO ligands. However, if the α QCC were only 0.64 MHz, then the observed T_1 for the α chains could be accommodated by a τ_c = 23 ns, the same as in HbCO A. Given the information currently available, we cannot differentiate between these two possibilities. However, since T_1 of the CO ligand of the rabbit Hb α chains is twice as large as that of human HbCO, while the *apparent* line width, which is dominated by the narrow component, is almost the same as that of human HbCO A, the 0.95-MHz QCC value seems more likely. If the longer T_1 relaxation time of rabbit Hb α chains resulted from the smaller ^{17}O QCC with the same τ_c as human Hb, the apparent line width of the ^{17}CO ligand of rabbit Hb α chains should be much smaller than that of human Hb, unless, of course, the CSA becomes larger and compensates for the line width decrease from the smaller ^{17}O QCC. The situation for rabbit HbCO is clearly complex and at present does not seem resolvable.

Conclusions

Our results yield the rotational correlation times of the CO ligands bound to various hemoproteins and thus allows us to investigate the motional aspects of CO in the heme pocket. In this context it is of interest to note the results of Marshall et al.[38], who have suggested significantly more motion for the metalloporphyrin in Hb than in Mb. On the basis of time-differential perturbed γ-ray angular correlation (PAC), the rotational correlation time for indium-111 in apohemoglobin with [^{111}In]-protoporphyrin IX is 23 ns, which is the same as our value for human HbCO A. For similarly reconstituted Mb,[39] PAC measurements yield τ_c = 16 ns. Since the PAC ratio, τ_c(Hb)/τ_c(Mb) = 1.4, is much less than the rigid-sphere ratio, τ_c(Hb)/τ_c(Mb) = 4.0, expected for both macromolecules tumbling as a whole, Marshall et al. have suggested that the metalloporphyrin exhibits

(35) Lee, H. C.; Gard, J. K.; Brown, T. L.; Oldfield, E. *J. Am. Chem. Soc.* **1985**, *107*, 4087.
(36) Marshall, A. G.; Bruce, R. E. *J. Magn. Reson.* **1980**, *39*, 47.
(37) Stryer, L. *J. Mol. Biol.* **1965**, *13*, 482.
(38) Marshall, A. G.; Lee, K. M.; Martin, P. W. *J. Chem. Phys.* **1983**, *78*, 1528.
(39) Marshall, A. G.; Lee, K. M.; Martin, P. W. *J. Am. Chem. Soc.* **1980**, *102*, 1460.

significantly more internal motional freedom in Hb than in Mb. Our results show a similar ratio, $\tau_c(Hb)/\tau_c(Mb) = 1.6$, very close to the PAC ratio of 1.4, supporting Marshall's hypothesis. This hypothesis of more motional freedom in HbCO A is significant in that it could originate from a more open heme pocket and result in a less hindered Fe–CO structure and higher CO binding affinity. Indeed, the CO binding affinity of human Hb in the R quaternary state is 4 times greater than that of Mb.[7] (Note that the ^{17}O NMR is probing the R conformation of Hb.) A recent structural analysis[5] also reveals a bent Fe–CO structure, where the bend angles are 165° and 150° for human HbCO and MbCO, respectively, which is consistent with our result of a less hindered HbCO structure.

Our results also provides some evidence on the role of the protein in regulating the CO ligand binding affinities of hemoproteins, especially in solution. We believe an important result emerging from this work is that the size of the heme pocket determines the ligand binding affinities, at least for the CO ligand, of hemoproteins. All of the proteins studied exhibit basically rigid Fe–CO units; however, the motional freedom of the Fe–CO units is different for the different hemoproteins. Thus the hemoproteins with the more open heme pocket provide more room for the CO ligand and/or the heme–CO unit, so they exhibit a less hindered Fe–CO structure (X-ray correlation) and show higher CO binding affinities (Table I).

These results can be summarized as follows: *Picket fence porphyrin*: $\delta_i = 376$, $\nu_{CO} = 1967$ cm^{-1}, linear Fe–C–O, unhindered "pocket", irreversible CO binding. *HbCO A α,β chains* (*and rabbit HbCO β chains*): $\delta_i = 369$, $\nu_{CO} = 1951$ cm^{-1}, 165° Fe–C–O bond angle, relatively mobile CO ligand, 0.004 Torr $P_{1/2}(CO)$. *Sperm whale MbCO*: $\delta_i = 366.5$, $\nu_{CO} = 1944$ cm^{-1}, 150° Fe–C–O bond angle, hindered/immobile CO "pocket", 0.018 Torr $P_{1/2}(CO)$. *Rabbit HbCO α chain*: $\delta_i = 361$, $\nu_{CO} = 1928$ cm^{-1}, rigid CO "pocket", weak CO bonding (in O_2-exchange experiments).

Thus stronger ligand bonding appears to correlate with a more deshielded chemical shift, a higher frequency IR CO stretch frequency, and a more linear Fe–C–O bond angle (where determined), due in large part, we believe, to the packing constraints imposed by the protein (or porphyrin) environment—the larger the constraints, the weaker the bonding, due to deviations from a linear Fe–C–O bond.

Acknowledgment. This work was supported in part by the U.S. National Institutes of Health (Grant HL-19481).

Resonance Raman Spectra of Nitridoiron(V) Porphyrin Intermediates Produced by Laser Photolysis

Wolf-Dieter Wagner and Kazuo Nakamoto*

Contribution from the Department of Chemistry, Todd Wehr Chemistry Building, Marquette University, Milwaukee, Wisconsin 53233. *Received August 22, 1988*

Abstract: Nitridoiron(V) porphyrins, NFeOEP (OEP, octaethylporphinato anion), NFeTPP (TPP, tetraphenylporphinato anion), and NFeTMP (TMP, tetramesitylporphinato anion), were produced by laser irradiation of thin films of the corresponding azido complexes at ~30 K. Formation of the nitrido complexes was detected by the appearance of the ν(Fe≡N) (ν, stretching vibration) at 876 cm^{-1} for the OEP and TPP complexes and at 873 cm^{-1} for the TMP complex in resonance Raman (RR) spectra. These assignments were confirmed by observed frequency shifts due to $^{56}Fe/^{54}Fe$ and $^{14}N/^{15}N$ isotopic substitutions. Frequencies of structure-sensitive bands known for OEP and TPP complexes suggest the Fe(V) state for the nitrido complex and rule out the possibility of π-cation-radical formation. Although the spin state cannot be determined definitively by vibrational spectroscopy, the relatively small Fe≡N stretching force constant (5.07 mdyn/Å) favors the high-spin $(d_{xy})^1(d_{xz})^1(d_{yz})^1$ configuration that was found for isoelectronic oxomanganese(IV) porphyrins. In the case of the OEP complex, RR spectroscopy provides evidence for a reaction scheme in which $NFe^{V}OEP$ is first formed by laser photolysis of the $N_3Fe^{III}OEP$ complex due to low-power irradiation (1–60 mW in the 406.7–514.5-nm range) and subsequently converted to the μ-nitrido dimer $(FeOEP)_2N$ by local heating, which occurred when high laser power (220 mW at 413.1 nm) was applied to the sample. This dimer exhibits the symmetric Fe–N–Fe stretching band at 438 cm^{-1}, which shows expected shifts upon $^{56}Fe/^{54}Fe$ and $^{14}N/^{15}N$ substitutions. Formation of the μ-nitrido dimer is also confirmed by the positions of the structure-sensitive bands in the high-frequency region. The above reaction scheme resembles the autoxidation process of oxyiron porphyrins at low temperature which yields ferrylporphyrins as the intermediate and the μ-oxo dimer as the final product at room temperature.

Extensive research in the past decades has revealed that nature relies on high-valent metalloporphyrins in a number of enzyme-directed processes of biological systems.[1,2] For example, oxygenation reactions catalyzed by cytochrome P-450[3-5] or horseradish peroxidase (HRP)[6,7] involve porphyrin intermediates that contain oxidation states higher than Fe(III). It is generally accepted that the active site of these intermediates is a ferryl moiety (Fe^{IV}=O). Interestingly, the first observation of the ferryl stretching vibration [ν(Fe=O), 852 cm^{-1}] was made for a model compound, O=FeTPP (TPP, tetraphenylporphinato anion)[8,9] by using resonance Raman (RR) spectroscopy. Subsequently, spectroscopic evidence of ferryl formation was obtained via observation of the ν(Fe=O) at 779 cm^{-1} for HRP-II[10,11] and at 797 cm^{-1} for myoglobin.[12] Other high-valent iron porphyrins reported thus far include nitrogen[13] and carbon-bridged[14] dimers which have been proved to

(1) Hewson, W. D.; Hager, L. P. In *The Porphyrins*; Dolphin, D., Ed.; Academic Press: New York, 1979; Vol. 7, pp 295–332.
(2) Griffin, B. W.; Peterson, J. A.; Eastbook, R. W. In *The Porphyrins*; Dolphin, D., Ed.; Academic Press: New York, 1979; Vol. 4, pp 179–256.
(3) Dawson, J. H.; Eble, K. S. *Cytochrome P-450: Heme Iron Coordination Structure and Mechanisms of Action*; Academic Press: New York, 1986; Vol. 4, pp 1–64.
(4) Lewis, D. F. V. *Drug Metab. Rev.* **1986**, *17*, 1–66.
(5) Alexander, L. S.; Goff, H. M. *J. Chem. Educ.* **1982**, *59*, 179–182.
(6) Harami, T.; Maeda, Y.; Morita, Y.; Trautwein, A.; Gonser, U. *J. Chem. Phys.* **1977**, *67*, 1164–1169.
(7) Hanson, L. K.; Chang, C. K.; Davis, M. S.; Fajer, J. *J. Am. Chem. Soc.* **1981**, *103*, 663–670.
(8) Bajdor, K.; Nakamoto, K. *J. Am. Chem. Soc.* **1984**, *106*, 3045–3046.
(9) Proniewicz, L. M.; Bajdor, K.; Nakamoto, K. *J. Phys. Chem.* **1986**, *90*, 1760–1766.
(10) Sitter, A. J.; Reczek, C. M.; Terner, J. *J. Biol. Chem.* **1985**, *260*, 7515–7522.
(11) Hashimoto, S.; Tatsuno, Y.; Kitagawa, T. *Proc. Natl. Acad. Sci. U.S.A.* **1986**, *83*, 2417–2421.
(12) Sitter, A. J.; Reczek, C. M.; Terner, J. *Biochim. Biophys. Acta* **1985**, *828*, 229–235.
(13) Summerville, D. A.; Cohen, I. A. *J. Am. Chem. Soc.* **1976**, *98*, 1747–1752.

0002-7863/89/1511-1590$01.50/0